Journal of Asian Concrete Federation
Vol. 1, No. 1, pp. 37-46, Sep. 2015
ISSN 2465-7964 / eISSN 2465-7972
http://dx.doi.org/10.18702/acf.2015.09.1.37

Ductile fiber wrapping for seismic retrofit of reinforced concrete columns

Donguk Choi*; S. Vachirapanyakun; S.-Y. Kim; and S.-S. Ha

(Received: July 1, 2015; Accepted: August 12, 2015; Published online: September 30, 2015)

Abstract: An experimental study was performed on fiber wrapping to strengthen RC columns with insufficient moment capacity and ductility. In pseudo-seismic test of four columns with a circular cross section, the test variable was fiber type: none, carbon fiber (CF), polyethylene terephthalate (PET), and combined use of CF+PET. PET has high tensile strength and ductility, but very low elastic modulus. While a large area of PET typically needs to be used, the amount of PET actually utilized was about 50% of CF in terms of fiber axial stiffness (E_fA_f). All columns wrapped by CF and/or PET showed significantly improved strengths over the control column (121~143% of control column) while ductility also significantly improved (2.3~3.1 times the control column). Performance of PET was comparable to that of CF in terms of strength and ductility improvement while no sign of fiber rupture was observed at ultimate stage due to excellent ductility intrinsic with PET.

Keywords: carbon fiber, polyethylene terephthalate, seismic retrofit, moment capacity, ductility.

1. Introduction

Carbon fiber has been often used for seismic retrofit of RC columns in Korea since 1990s. Seismic design was first introduced to Korean Building Code in 1980s and many RC columns constructed before the introduction of the seismic design provisions lack flexural strength and ductility. Carbon fiber has excellent mechanical properties including strength and stiffness while durability characteristics are also excellent. [1] The fracture strain of CF in tension, however, is typically on the order of 1% which can be a severe drawback for CF to be used for fiber wrapping for the purpose of seismic retrofit of RC columns which typically experience large deformation under strong seismic activities. Ductile polyethylene terephthalate (PET) wrapping for seismic retrofit of RC columns was explored in this study. PET is typically used in construction as geotextile fabric in Korea in the form of thin bi-axially woven sheet.

Corresponding author Donguk Choi is a Professor of Dept. of Architectural Engineering at Hankyong National University, Anseong, Korea.
S. Vachirapanyakun is a M.S. student of Graduate School of Architecture of Hankyong National University, Anseong, Korea.
S.-Y. Kim is a M.S. student of Graduate School of Architecture of Hankyong National University, Anseong, Korea.
S.-S. Ha is an Associate professor of Kangnam University, Yongin, Korea.

PET has tensile strength over 600 MPa, high fracture strain on the order of 15%, but very low elastic modulus smaller than 1/20th of steel. It is noted that the PET was first applied for seismic retrofit of RC columns in Japan. Aggawidjaja et al. tested 14 shear deficient RC columns with rectangular cross-sections wrapped using carbon fiber (CF), aramid fiber (AF), polyethylene naphthalate (PEN), and PET. Both shear capacity and ductility increased compared to the control specimen. Aggawidjaja et al. proposed a mathematical model to predict the pier deformation capacity based on the experimental results. [2] Chun et al. performed an experimental study on seismic retrofit of rectangular columns using two to three layers of CF. Chun et al. reported that the strength of CF wrapped columns increased by 46 ~ 59% while ductility also increased significantly over the control column. [3]

2. Preparation for pseudo-dynamic test of RC columns

2.1 Mechanical properties of fibers

The mechanical properties of CF and PET in tension were first determined using 500-N capacity LR5K UTM by Lloyd Instrument. Results of tensile test performed following ISO 10406-2 are summarized in Table 1 and Fig. 1. [4] As shown in Table 1 and Fig. 1, CF has much higher strength

and elastic modulus than PET, but PET can develop much larger strain than CF. It is also shown in Fig. 1 that the stress-strain relationship of CF is linear while it is non-linear for PET. A two-part epoxy was used to provide bond between fibers and concrete in this study while the mechanical properties of the adhesive (called K2 hereinafter) is also included in Table 1.

2.2 Fabrication of column test specimens

The column cross sections were designed using low strength concrete and reinforcement in this study to reflect the common practice in Korea in the 1980s. Table 2 summarizes test variables. Table 3 summarizes the mechanical properties of column reinforcement. The stress-strain relationship was measured in the laboratory and recorded both for concrete and reinforcement, and later used for moment-curvature analyses of the column cross sections.

All RC columns had a circular cross section with a diameter of 400 mm. The column test specimens were cast in two parts: column stub and column. Column main bars (SD300 Grade 12 D16) were extended from the column stub into the columns without any splices. D10 column ties were used at 250 mm o.c. All column sections were designed to have sufficient shear resistance so that the columns would fail in flexure. All columns were cast in paper mold. The paper mold was removed after one day and the columns were wet cured for seven days using plastic sheet.

Before fiber wrapping, the concrete surface was lightly ground using a hand grinder to improve bond. Except for the control column (C-Control), fibers were wrapped around the column for the height of $2d$ (d = 352 mm, effective depth) above the column stub completely surrounding the plastic hinge zone. For C-PET, multiple layers of bi-axially-woven PET sheet were used.

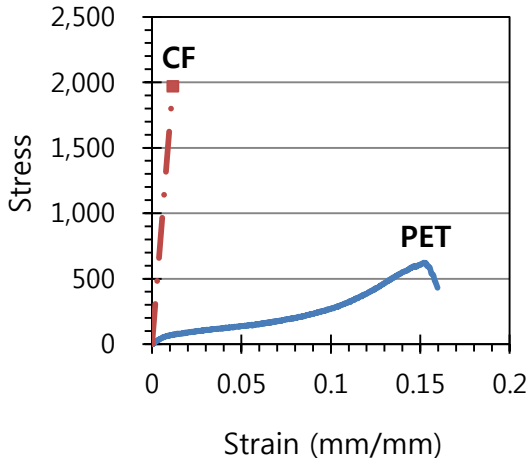

Fig. 1 – Stress- strain relationship of CF vs. PET

Table 1 – Mechanical properties of fibers and adhesive

Fiber type	Tensile strength (MPa)	Maximum strain in tension	Elastic modulus (GPa)	Cross-sectional area (mm^2)	Thickness (mm)	Density (g/mm^3)
CF roving	1,970	0.0116	169.00	0.446 1)	0.109	0.00180
PET sheet	613	0.1495	7.10 3)	5.250 2)	0.106	0.00140
K2 (adhesive)	40.9	0.0258	1.59	4)	--	--

Notes: 1) Cross-sectional area of a CF roving; 2) cross-sectional area of bi-axial PET sheet per 100-mm width (area of fibers in the axial direction only is given); 3) secant modulus corresponding to 1% strain; 4) volume of adhesive used is 200% of fiber by vol., typ.

Table 2 – Summary of concrete strengths and test variables

Column index	f_{ck} (MPa)	ρ_{st} (%)	ρ_{tie} (%)	ρ_f (%)	Fiber wrapping scheme
C-Control	21.0	1.93	0.37	--	
C-CF				0.108	CF 1 layer, A_{CF} = 21.2 mm^2/pitch 1)
C-PET				1.050	PET 20 layers, A_{PET} = 263 mm^2/pitch
C-HF				1.080	PET 20 layers + CF strips 2)

Notes: 1) 1 pitch = 250 mm, typ. (tie spacing); 2) CF strip cross-sectional area is 7.96 mm^2/pitch for C-HF.

Table 3 – Mechanical properties of column reinforcement

Reinforcement	f_y (MPa)	f_{ult} (MPa)	E_s (GPa)
Main bar, 12 D16	347	522	178
Tie, D10 @ 250 o.c.	465	718	181
Column stub, D25	548	--	--

For C-CF, uniaxial CF sheet with mechanical properties similar to fiber rovings as shown in Table 1 were used. The amount of fiber wrapping was one layer of CF sheet for C-CF and 20 layers of PET sheet for C-PET, respectively. Many layers of PET sheet were needed due to low elastic modulus of PET. It is noted that, after fiber wrapping, $E_{PET}A_{PET}$ was 52% of $E_{CF}A_{CF}$ in terms of axial stiffness. For the C-HF, in addition to 20 layers of PET sheet, CF strips were wrapped at 150 mm o.c. Fig. 2 shows three columns after fiber wrapping.

2.3 Instrumentation, test method, and measurementation

Columns were heavily instrumented as shown in Fig. 3. Three sets of strain gauges were installed on two main reinforcing bars located at North/South (N/S) and subjected to maximum +/- moment, respectively, to measure flexural strains. Two sets of strain gauges were installed on ties at East/West (E/W), respectively, to measure hoop strains. In addition, two sets of strain gauges were installed on fibers to measure fiber strains at E/W, respectively. The locations of strain gauges installed on fibers were at half point vertically between the strain gauge locations installed on column ties. A total of seven linear variable displacement transducers (LVDTs) were used to measure displacement of the column and the column stub.

Lateral force H was applied at 1.2 m (half a story height in about 2/3rd of full scale) above the top surface of column stub using a 1,200-kN capacity Instron PL 1.0N actuator while the concentric axial force P was applied on top of the column using a 2,000-kN hydraulic cylinder operated by a hand pump. Force applied by the hydraulic cylinder was carefully monitored using pressure transducer during test to constantly maintain a vertical force of 350 kN (about 10% of column axial capacity) which simulated dead load. All data were electronically monitored and stored using a TDS 530 data logger.

Pseudo-dynamic tests were carried out generally following procedures suggested in ref. [5]. Displacement control for the lateral force application was adopted and is shown in Fig. 4. As shown in Fig. 4, the same displacement cycle was repeated for two times. The typical displacement cycle was 1, 2, 3, 4.5, 6, and 8Δ_y while Δ_y was taken as an average value of the displacements at the first yielding of the main reinforcing bar located at N/S. Test was terminated when the maximum lateral load of a specific cycle dropped below 80% of the maximum lateral load recorded for the specific column specimen.

3. Results of RC column test

3.1 Hysteretic behavior

The column tests consisted of four columns: a Control column (C-Control), a CF strengthened column (C-CF), a PET strengthened column (C-PET), and a hybridized PET+CF strengthened column (C-HF). Table 4 summarizes the test results in terms of moment and displacement values at limiting states, ductility, and failure modes while Fig. 5 shows the hysteretic curves of all columns determined from tests.

It is seen in Fig. 5 that C-CF, C-PET, and C-HF reached significantly higher peak loads with increasingly larger displacements than C-Control. At yield stage, M_y of C-CF, C-PET, and C-HF are 109%, 112%, and 118% of $M_{y\text{-}Control}$, respectively. At peak, M_{max} of C-CF, C-PET, and C-HF are 121%, 128%, and 143% of $M_{max\text{-}Control}$, respectively, in Table 4.

Displacement ductility can be defined as a displacement at failure (at a specific cycle where the peak load of the cycle dropped below the max. load recorded for the specimen) over a displacement at yield. Displacement ductility of C-CF, C-PET, and C-HF over C-Control is 2.26, 3.06, and 3.06, respectively, in Table 4. Drift ratios, Δ_{max}/1,200 (shear span = 1,200 mm in Fig. 3), are 4.2, 6.5, 8.0, and 8.9 for C-Control, C-CF, C-PET, and C-HF, respectively.

Fig. 6 shows envelops of the hysteretic curves of all four columns. Fig. 6 reveals that the highest moment and displacement were achieved by C-HF. Behaviors of C-CF and C-PET are similar and are significantly superior to that of C-Control both in terms of moment and displacement. The test results clearly show the effectiveness of both CF and PET wrapping in increasing the moment capacity and the ductility over the Control column. It is noted that test data are shown only for the first quadrant for C-CF in Fig. 6. This is due to a mistake in manipulation of the actuator during testing C-CF. In a specific cycle, the actuator went to into much larger displacement than a planned value by a handling mistake and partial fracture of CF occurred in one face (S) of the column at the maximum moment region. This partial failure of CF did not seem to have affected the behavior in the opposite loading direction (N), fortunately, and test of C-CF continued with results shown in Figs. 5 through 7.

3.2 Energy dissipation

The area under respective loop of the hysteretic curve represents the energy dissipation of the specific cycle and is shown in Fig. 7 for all columns. Fig. 7 indicates that the areas under each loop are

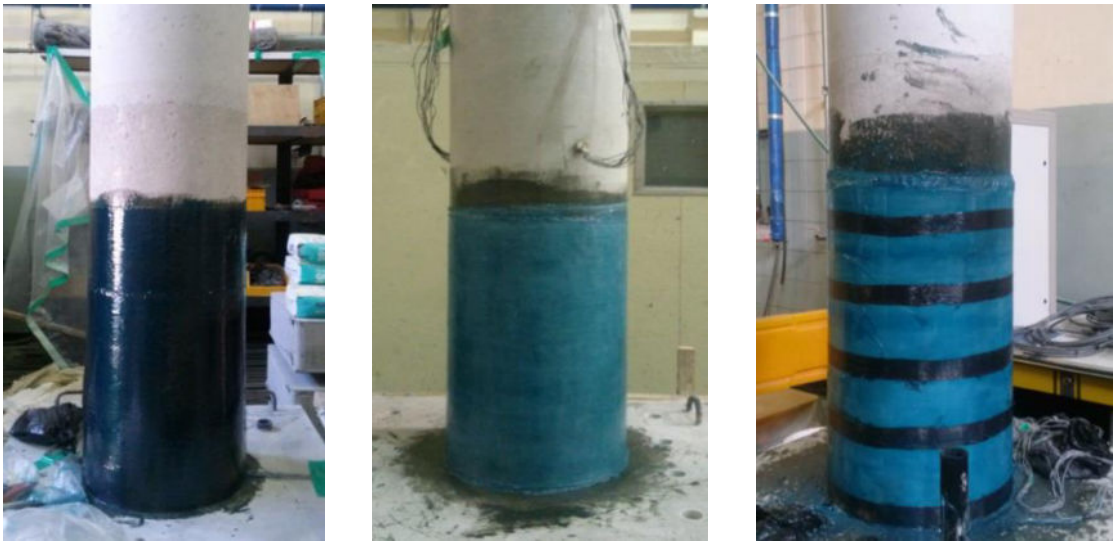

(a) C-CF (b) C-PET (c) C-HF (PET+CF)

Fig. 2 – Fiber wrapped RC columns

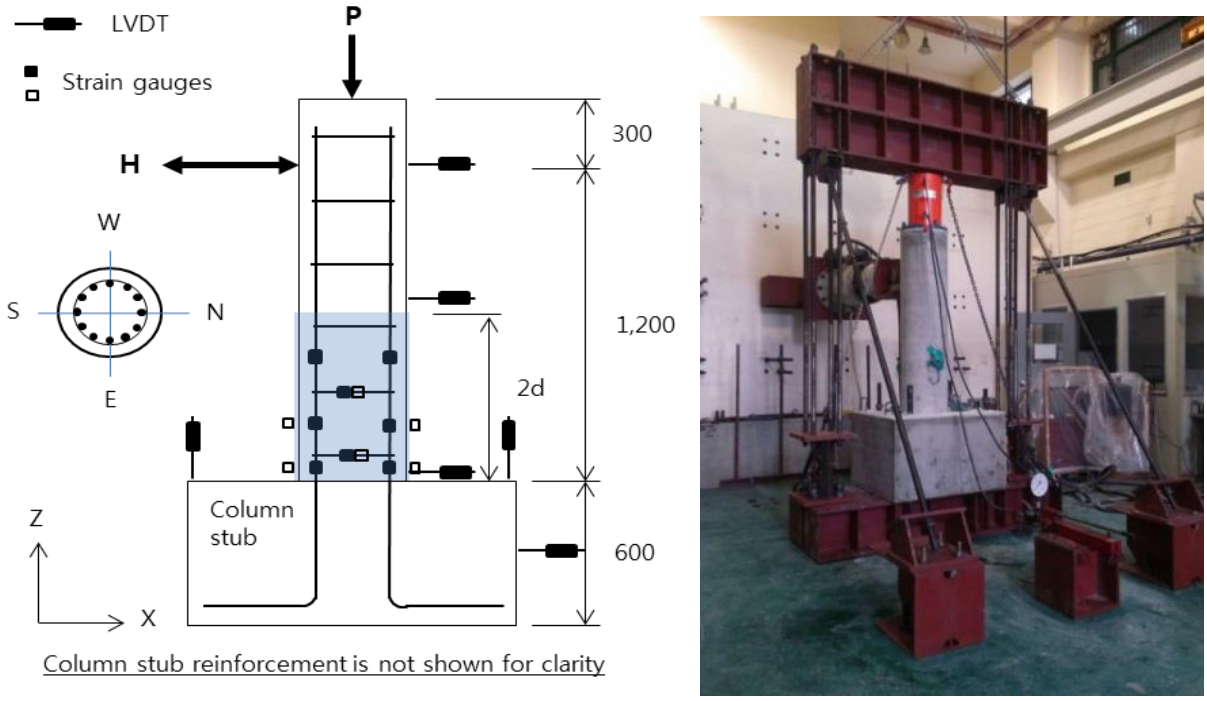

Fig. 3 – Column test setup

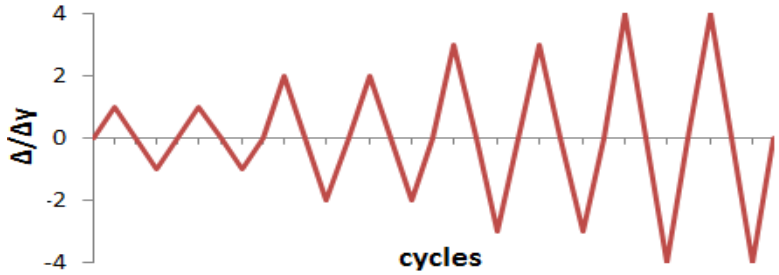

Fig. 4 – Program for lateral force application

similar among C-Control and C-CF, C-PET or C-HF in the beginning, but the energy dissipation significantly increases in C-CF, C-PET, and C-HF and reaches over 200% of C-Control at the end. Fig. 7 also reveals that energy dissipations by C-PET and C-HF are larger than C-CF. It needs to be noted that the energy dissipation capacity of C-HF of the last loop is smaller than that of a loop just before the last cycle. This is because of the CF fracture that occurs in the cycle just before the last cycle as

shown in Fig. 5 (d). After loss of extra confinement by CF, the confinement is provided only by PET which results in decreased energy dissipation for the last loop in Fig. 7.

3.3 Failure mode

As shown in Table 4 and Fig. 8 (a), C-Control failed as the main reinforcing bars buckled following the loss of concrete cover in the plastic hinge zone. C-CF failed by rupture of CF at measured maximum fiber strains of about 1.1% followed by buckling of the column main bars as shown in Fig. 8 (b). On the other hand, the failure mode of C-PET was the tensile failure of the main reinforcing bars following the loss of concrete cover and the main bar buckling as shown in Fig. 8 (c). The main bars first buckled then the buckled bars ruptured in tension during subsequent reloading in the opposite direction. It is also important to note that in all PET-strengthened columns (C-PET and C-HF), PET remained undamaged which again demonstrated the excellent ductile characteristics. In C-HF, wrapped by CF strips in addition to PET sheet, the CF strip at the maximum moment region ruptured first at the maximum load, but the load resisting capacity of C-HF was not suddenly lost as PET helped keep providing column with resistance.

3.4 Load vs. strains: column ties and fiber strain

3.4.1 Strains in column ties

Fig. 9 shows load vs. strain values developed in column ties during test where tie level 1 represents the tie closest to column stub and so on. Fig. 9 shows that the tie strains developed in the fiber wrapped columns are larger than those of the control column and the maximum tie strain (average value of E/W) is on the order of 0.15% and therefore the ties do not reach the yield point in all columns.

3.4.2 Fiber strains

Fig. 10 (a) shows that the maximum fiber strain in the hoop direction is close to 0.6% for C-CF and it is about 1% for C-PET, respectively. It needs to be noted that, unlike strains measured on the column ties, the strain values developed in continuously applied fibers can be much larger than that shown in Fig. 10 (a). For example, for C-CF, CF must have ruptured at about 1.16% strain during test (the rupture strain of CF is 1.16% as shown in Table 1), but Fig. 10 (a) only shows the maximum strain value of about 0.6%. This argument should also be valid for the hoop strains shown for C-PET. Fig. 10 (b) shows that the maximum PET strain measured in the column axial direction is about 0.5% while it is expected that the actual PET strain in hoop direction has been much larger than 0.5%.

4. Theoretical interpretation of test results

4.1 Stress-strain relationship of confined concrete

It was desired to perform moment-curvature analyses of the column cross-sections to futher analyze the effectiveness of the different types of fiber wrapping. Complete stress-strain curves of the confined concrete are needed for this purpose and, in this study, the well known theoretical stress-strain model of confined concrete by Mander et al. was used. [6] As shown in Fig. 1, the stress-strain relationship of PET is non-linear. A numerical expression in the form of a polynomial equation was developed using the Method of Least Square to determine the best fit curve up to 4% strain of PET as shown in Fig. 11.

Table 4 – Summary of test results of RC columns

Column index	Moment		Displacement		Ductility and failure modes		
	M_y (kNm)	M_{max} (kNm)	Δ_y (mm)	Δ_{max} (mm)	Displ. ductility	Drift ratio (%)	Failure mode
C-Control	116	147	11.5	50.4	4.38	4.20	Column main bar buckling
C-CF	126	178	7.92	78.4	9.90	6.53	CF rupture
C-PET	130	188	7.18	96.1	13.4	8.01	Column main bar rupture
C-HF 1)	137	210	8.01	107	13.4	8.92	ditto

Notes: 1) End of actuator stroke was reached for C-HF during reverse cyclic loading. Test was stopped temporarily while the actuator stroke was readjusted. C-HF ultimately failed in shear under monotonic loading. Data given in Table 4 are for reverse cyclic loading only

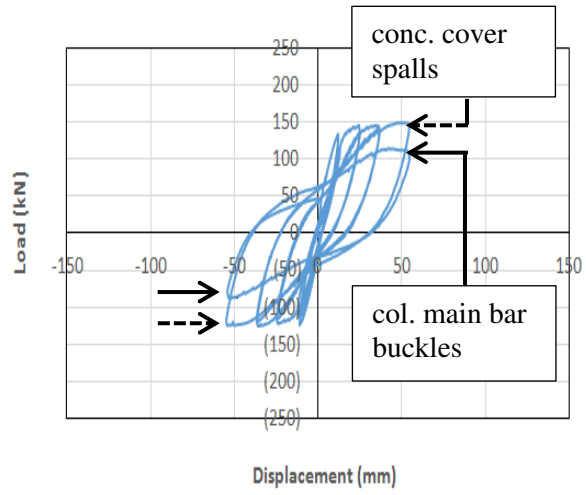

(a) C-Control

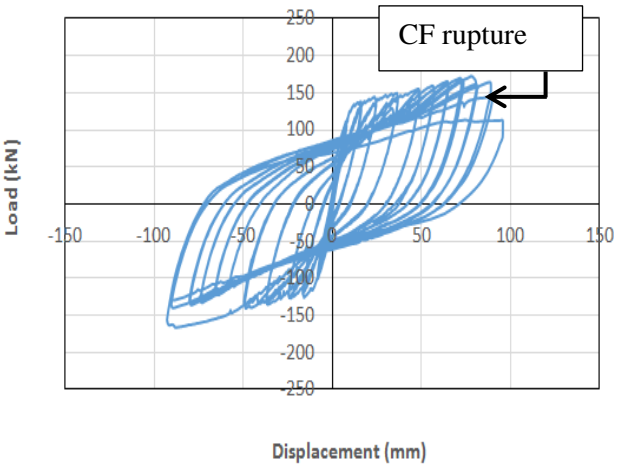

(b) C-CF

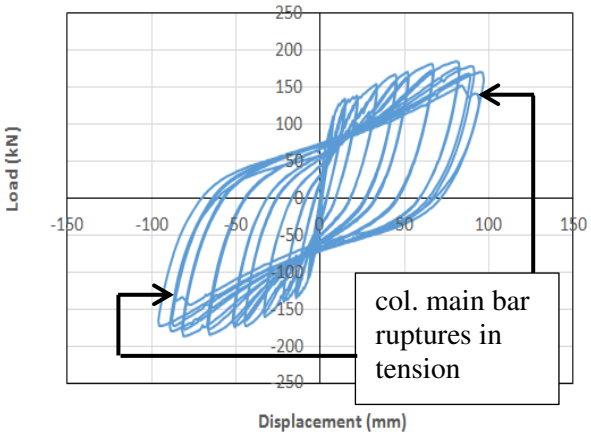

(c) C-PET

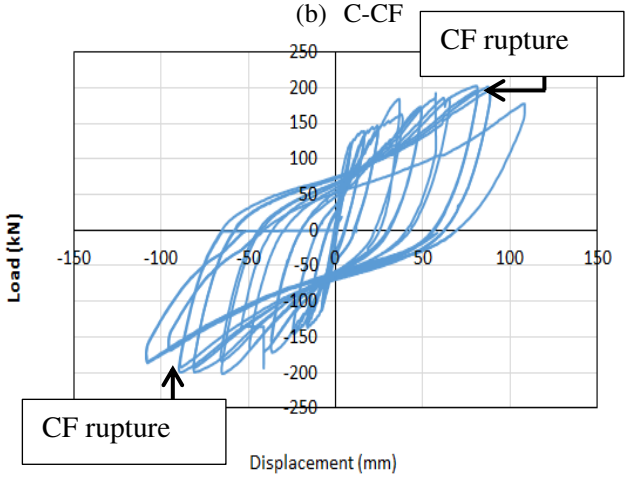

(d) C-HF (PET+CF)

Fig. 5 – Hysteretic behavior

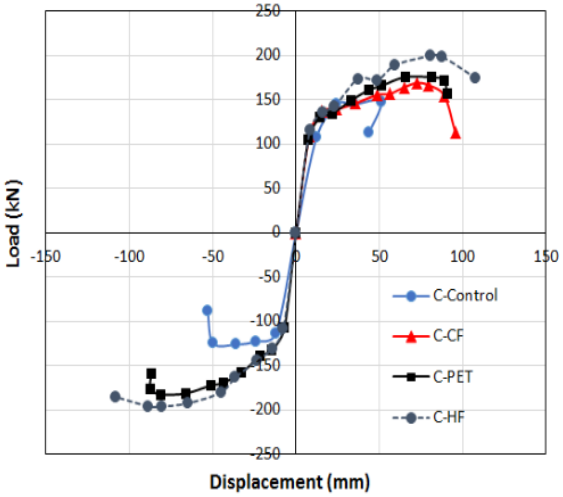

Fig. 6 – Envelop of hysteretic curves

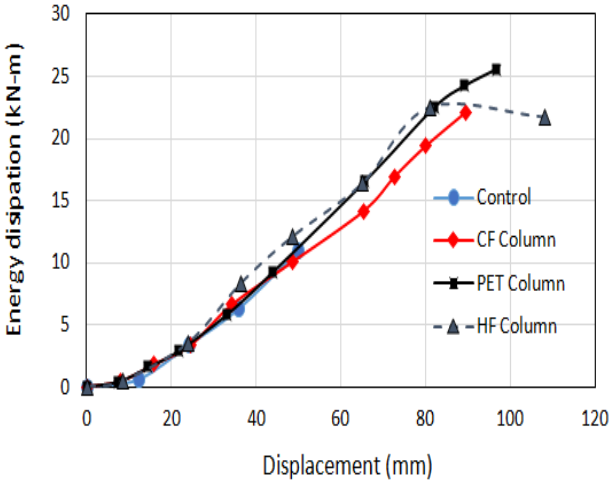

Fig. 7 – Energy dissipation

(a) C-Control (b) C-CF (c) C-PET

(d) C-PET (e) C-PET (f) C-HF (PET+CF)

Fig. 8 – Failure modes

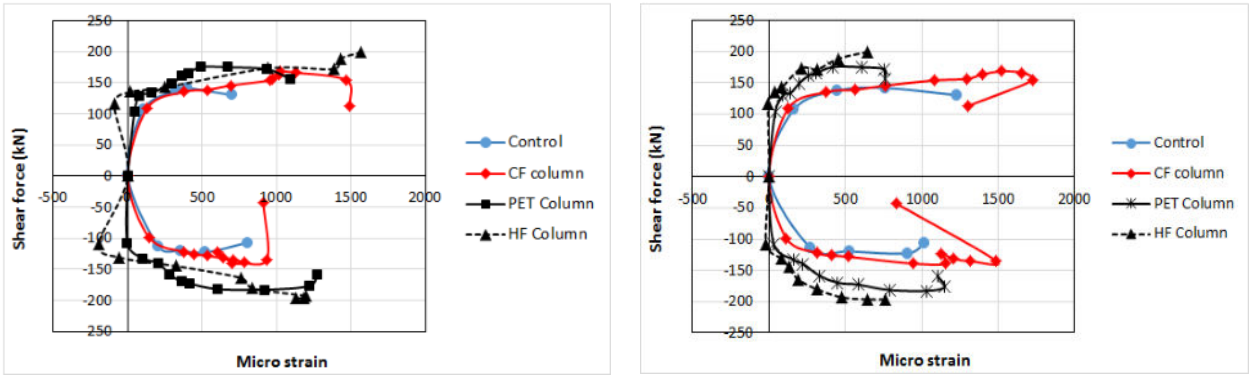

(a) Col. ties – level 1 (b) Col. ties – level 2

Fig. 9 – Load vs. column tie strains (E/W average value)

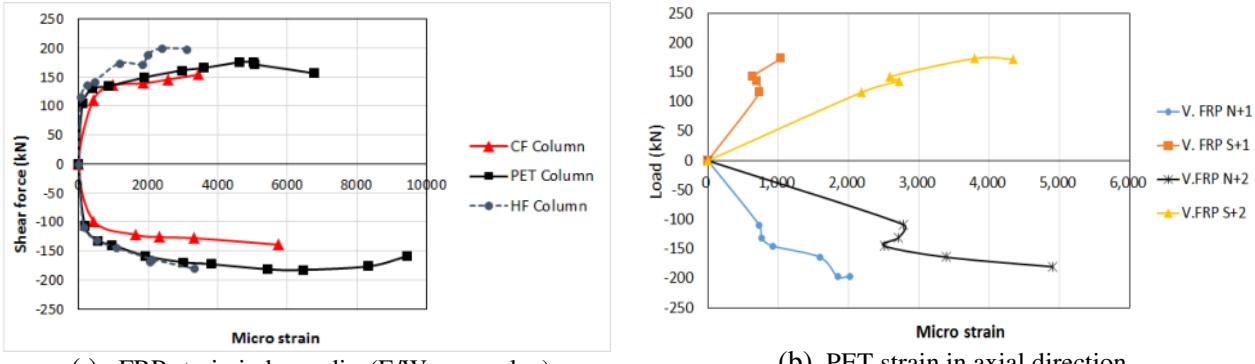

(a) FRP strain in hoop dir. (E/W avg. value) (b) PET strain in axial direction

Fig. 10 – Load vs. fiber strains

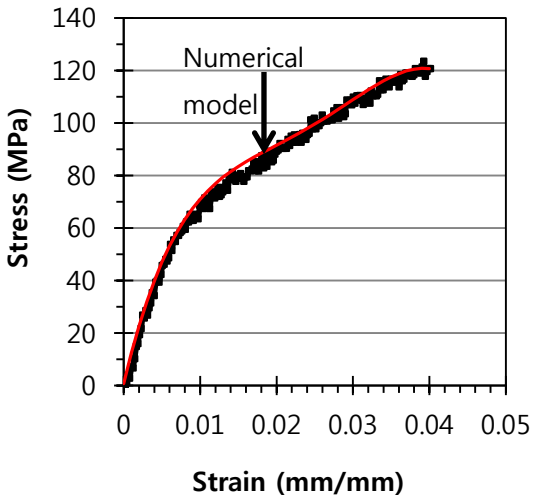

Fig. 11 – Curve fitting: PET stress-strain relationship up to 4%

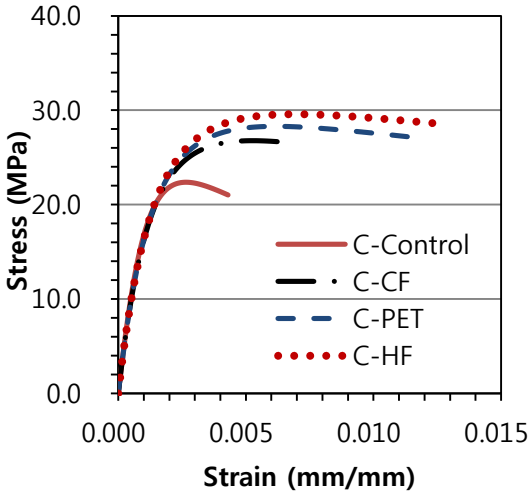

Fig. 12 – Stress-strain relationship of confined concretes [6]

The strength and the corresponding longitudinal strain at the strength of concrete confined by an active hydrostatic pressure can be represented by the following relationships:

$$f'_{cc} = f'_{co} + k_1 f_L \quad (1)$$

$$\varepsilon_{cc} = \varepsilon_{co}\left(1 + k_2 \frac{f_L}{f'_{co}}\right) \quad (2)$$

where f_{cc}' and ε_{cc} are the maximum concrete stress and the corresponding strain, respectively, under the lateral pressure f_L; f_{co}' and ε_{co} are unconfined concrete strength and corresponding strain, respectively; and k_1 and k_2 are coefficients that are functions of the concrete mix and the lateral pressure where, in this study, k_1 and k_2 are taken as 4.1 and 5 k_1, respectively. [6]

The lateral pressure can be determined using Eq. (3).

$$f_L = \frac{2E_f n t_f \varepsilon_{fe}}{D} \quad (3)$$

where E_f is elastic modulus of FRP, n = number of FRP layers, t_f is nominal thickness of one layer of FRP, ε_{fe} is effective strain of FRP at failure, and D is diameter of the circular column. [1]

In Eq. (3), the effective strain of CF is 1.16% as shown in Table 1 while it is rather arbitrarily set to be 3% for PET based on observations during tests. Complete stress-strain curves of the confined concrete can be now determined using stress-strain relationships of various confined concretes for the four different columns determined using Eqs. (1) ~ (3) and the procedure suggested in reference [6]. Fig. 12 shows the stress-strain relationships of various confined concretes for the four different columns determined using the above procedure.

4.2 Moment-curvature analyses of column cross sections

The moment–curvature analyses were performed on the column circular cross sections using the stress-strain curve of fibers shown in Fig. 1, the concrete stress-strain relationships shown in Fig. 12, and bi-linear model of stress-strain relationship of column main reinforcement (to reflect strain hardening effect). Analyses were performed either with or without considering the effect of axial fibers in case of bi-axially woven PET. Table 5 summarizes the results of the moment-curvature analyses. Table 5 also compares the theoretical values with the experimental results. In Table 5, the experimentally determined moments of C-Control both at yield and ultimate stages match very well with the theoretical moments. For C-CF, C-PET, and C-HF, the ratio of the theoretical moment over the experimentally determined moment is 0.931, 0.907, and 0.862 at yield stage while it is 0.88, 0.857, and 0.773 at ultimate stage. It is noted that the PET sheet used in this study is bi-axially woven while the amount of fibers running in the hoop direction and the axial directions are the same. Improved moment-curvature analyses also considering the fibers in the axial direction resulted in the ratio of theoretical over experimental moments at yield stage as 0.922 and 0.876, respectively, for C-PET and C-HF. The ratio is 0.904 and 0.813 at ultimate stage for C-PET and C-HF, respectively. The theoretical calculations considering non-linearity of PET, stress-strain behavior of confined concrete, and strain hardening of reinforcing steel in general can predict the test values well.

It should be noted that the amount of PET used is only 52% of CF in terms of fiber axial stiffness

(E_fA_f) as described previously. The ultimate moment capacity of C-PET, however, is higher than that for the C-CF as shown. This is due to the high strength and ultimate strain of concrete confined by PET as shown in Fig. 12.

Curvatures of the column section can be determined theoretically both at yield and ultimate stages. Table 5 shows that the curvature ductility (Φ_u/Φ_y) of C-Control, C-CF-, C-PET, and C-HF is 2.88, 5.12, 8.92, and 9.53, respectively. Again, while the fiber wrapping is effective in increasing the ductility of all RC column sections tested, it is more effective with the PET wrapping than the CF wrapping

Table 5 – Results of moment-curvature analyses vs. experimental results

Column index	Experimental values (kNm)		Theoretical values (M – kNm, Φ - 10^{-5} rad/mm)				$M_{y\text{-}calc}$ / $M_{y\text{-}test}$	$M_{u\text{-}calc}$ / $M_{u\text{-}test}$	Φ_u / Φ_y
			Yield stage		Ultimate stage				
	$M_{y\text{-}test}$	$M_{u\text{-}test}$	$M_{y\text{-}calc}$	Φ_y	$M_{u\text{-}calc}$	Φ_u	(%)	(%)	
C-Control	116	147	117	1.06	149	3.05	100	101	2.88
C-CF	126	178	117	1.05	156	5.39	93.1	88.0	5.12
C-PET 1) - hoop only - hoop+axial	130	188	118 120	1.05 1.05	161 170	9.59 9.41	90.7 92.2	85.7 90.4	9.14 8.92
C-HF 1) - hoop only - hoop+axial	137	211	118 120	1.05 1.05	163 172	10.2 10.0	86.2 87.6	77.3 81.3	9.80 9.53

Notes: 1) C-PET and C-HF: analyses first excluded the effect of fibers in the axial direction (i.e. considered hoop direction fibers only) and then included the effect of axial fibers of bi-axial PET sheet (both hoop direction and axial direction fibers).

5. Conclusions

While fiber wrapping has been done since 1990s in Korea, PET is new for application in RC structure. PET has high strength, very large fracture strain, and very low elastic modulus. A total of four columns including CF- and/or PET- wrapped RC columns and a control column was tested in this study with results summarized below.

(1) All columns wrapped by CF and/or PET showed significantly improved strengths over the control column: ultimate moments ranged between 121% and 143% of the control column.
(2) Performance of PET was at least comparable to that of CF in terms of strength and ductility improvement while no sign of fiber rupture was observed at ultimate stage due to excellent ductility intrinsic with PET.
(3) Although the amount of PET actually utilized was only 52% of CF in terms of fiber axial stiffness (E_fA_f), the ultimate moment of PET wrapped column was higher than that of CF wrapped column. This is due to the high strength and ultimate strain of concrete confined by PET as evidenced by theoretical calculation.
(4) Both CF and PET wrapping were effective in increasing the ductility of all RC column sections. Ductility of columns wrapped by CF and/or PET improved 2.3~3.1 times the control column. PET wrapping was more effective than the CF wrapping.

It must be noted that the durability characteristics of PET are currently under investigation for actual application of PET in the field. Due to very low elastic modulus of PET, a large amount needs to be utilized which leads to increased thickness. In this study, the thickness of 20 layers of PET along with adhesive was on the order of 6 mm. The bond characteristics between PET and concrete substrate must also be studied in the future.

Acknowledgements

This work was supported by CareCon Co. who supplied this research with materials and financial funding during the experimental phase of the study. Authors are grateful for the generous support.

References

1. ACI 440.2R-08 (2008) Guide for the Design and Construction of Externally Bonded FRP Systems for Strengthening Concrete Structures, ACI Com-

mittee 440, American Concrete Institute, Detroit, Michigan, 76 pp.
2. Aggawidjaja, D; Ueda, T.; Dai J.; and Nakai, H. (2006) "Deformation capacity of RC piers wrapped by new fiber-reinforced polymer with large fracture strain," Cement and Concrete Composites, 28, pp. 914~927.
3. Chun S.-C.; Park H.-C.; Ahn, J.-H.; and Park C.-L. (1999) "Behavior of Concrete Columns Confined by Carbon Fiber Sheets under a Constant Axial Force and with Reversed Cyclic Lateral Loading," KCI Journal, Korea Concrete Institute, 11(2), pp. 147~156 (*in Korean*).
4. ISO 10406-2 (2015) Fibre-reinforced polymer (FRP) reinforcement of concrete – Test methods – Part. 2: FRP sheets, Geneva, Switzerland.
5. ACI 374.2R-13 (2013) Guide for Testing Reinforced Concrete Structural Elements under Slowly Applied Simulated Seismic Loads, ACI Committee 374, American Concrete Institute, Detroit, Michigan, 18 pp.
6. J.B. Mander; M.J.N. Priestly; and R. Park (1988) "Theoretical Stress-Strain Model for Confined Concrete," ASCE Journal of Structural Engineering, American Society of Civil Engineering, pp. 1804-1826.
7. ACI 440.1R-03 (2003) Guide for the Design and Construction of Concrete Reinforced with FRP bars, ACI Committee 440, American Concrete Institute, Detroit, Michigan, 42 pp.
8. Elwood K. J. and Eberhard M. O. (2009) "Effective Stiffness of Reinforced Concrete Columns," ACI Structural Journal, 106(4), pp. 476-484.
9. Park R. and Paulay T. (1975) Reinforced Concrete Structures, John Wiley and Sons, 1975.